Development of a Novel Supervisory Controller on a Parallel-Hybrid Powertrain for Small Unmanned Aerial Systems

Lionel Fouellefack, Lelanie Smith,
Department of Mechanical and Aeronautical Engineering, University of Pretoria, Pretoria, South Africa
Michael Kruger
Department of Aerospace and Mechanical Engineering, University of Southern California, California, USA

Abstract

Purpose – A Hybrid-Electric Unmanned Aerial Vehicle (HE-UAV) model has been developed to address the problem of low endurance of a small electric UAV. Electric powered UAVs are not capable of achieving a high range and endurance due to the low energy density of its batteries. Alternatively, conventional UAVs (cUAVs) using fuel with an internal combustion engine (ICE) produces more noise and thermal signatures which is undesirable especially if the air vehicle is required to patrol at low altitudes and remain undetected by ground patrols. This work investigates the impact of implementing hybrid propulsion technology to improve on the endurance of the UAV (based on a 13.6 kg UAV).

Design/methodology/approach – A HE-UAV model is developed to analyze the fuel consumption of the UAV for given mission profiles which was then compared to a cUAV. Although, this UAV size was used as reference case study, it can potentially be used to analyze the fuel consumption of any fixed wing UAV of similar take-off weight. The model was developed in a Matlab-Simulink environment using Simulink built-in functionalities, including all the subsystem of the hybrid powertrain. That is, the ICE, electric motor, battery, DC-DC converter, fuel system and propeller system as well as the aerodynamic system of the UAV. Additionally, a ruled based supervisory controlled strategy was implemented to characterize the split between the two propulsive components (ICE and electric motor) during the UAV mission. Finally, an electrification scheme was implemented to account for the hybridization of the UAV during certain stages of flight. The electrification scheme was then varied by changing the time duration of the UAV during certain stages of flight and comparisons were made between the UAV in electric mode and cUAV on the fuel consumption during each mission.

Findings – Based on simulation, it was observed a HE-UAV could achieve a fuel saving of 33 % compared to the cUAV. A validation study showed a predicted improved fuel consumption of 9.5 % for the Aerosonde UAV.

Originality/value – The novelty of this work comes with the implementation of a rule-based supervisory controller to characterise the split between the two propulsive components during the UAV mission. Also, the model was created by considering steady flight during cruise, but not during the climb and descend segment of the mission.

Papertype – Research paper

Thecurrentissueandfulltextarchiveofthisjournalisavailableon Emerald Insight at: https://www.emerald.com/insight/1748-8842.ht

Aircraft Engineering and Aerospace Technology

Nomenclature
Symbols

M_0 = Motor Shaft Torque (Nm);

Q_m = Motor Torque Constant (Nm/A);

V = Motor Voltage (V);

P_m = Motor Shaft Power (W);

P_{in} = Electric Input Power (W);

η_m = Mechanical Efficiency;

η_g = Generator Efficiency;

J = Advance Ratio;

D_p = Propeller Diameter (m);

n = Rotational Speed (rev/s);

V = Propeller Speed (m/s);

P_A = Propeller Available Power (W);

T = Propeller Torque (N);

C_T = Thrust Coefficient;

C_P = Power Coefficient;

I_m = Motor Current (A);

r_m = Motor Internal Resistance (Ω);

I_0 = Zero Torque Current (A);

U_m = Motor Terminal Voltage (V);

η_p = Propeller Efficiency;

K_v = Motor Speed Constant (rpm/V);

V_m = Motor Internal Back EMF (V);

Ω = Motor Rotational Speed (Rev/s);

V_{park} = Battery Pack Voltage (V);

Q_{park} = Battery Pack Capacity (C);

N_{cells} = Number of Battery Cells;

V_{cell} = Battery Cell Voltage (V);

Q_{cell} = Battery Cell Capacity (C);

m_{fuel} = Fuel Mass (Kg);

$\dot{m}_{fuel}$ = Fuel Mass Flow Rate (kg/s);

D = Drag Force (N);

α_T = Climb Angle (deg);

$T_r = Propeller\ Thrust(N)$;

T = Thrust Force (N);

SFC = Specific Fuel Consumption (kg W^1 s^1);

R = Motor Resistance (Ω);

W = Weight (N);

L = Lift (N);

ρ = Density (kg/m^3);

S_w = Reference Area (m^2);

C_D = Drag Coefficient;

C_L = Lift Coefficient;

T_{ICE} = ICE Torque (Nm);

T_{EM} = EM Torque (Nm);

P_{ICE} = ICE Power (W);

P_{EM} = EM Power (W);

HF = Hybridization Factor;

Ω = Rotational Speed (rad/s);

P = Pressure (N/m^2);

T = Temperature (K);

BSFC = Brake Specific Fuel Consumption (kg/wh);

T_r = Motor Torque Constant (N);

η_{th} = Engine Throttle;

P_{atm} = Atmospheric Presssure (Pa);

P_{min} = Minimum Atmospheric Presssure (Pa);

K_Q = Motor Torque Constant (Nm/A);

P_M = Mission Power (W);

T_M = Mission Torque (Nm);

FF_M = Mission Engine Fuel Flow (kg/s);

$BSFC_M$ = Mission Specific Fuel Consumption (g/wh);

Definitions, acronyms and abbreviations

BSFC = Brake Specific Fuel Consumption;
ICE = Internal Combustion Engine;
UAV = Unmanned Aerial Vehicle;
HE-UAV= Hybrid Electric Unmanned Aerial Vehicle;
HEPS = Hybrid Electric Propulsion System;
HF = Hybridization Factor;
MPC = Model Predictive Control;
ECMS = Equivalent Consumption Minimization Strategy;
CMAC = Cerebella Model Arithmetic Computer;
ANN = Artificial Neural Network;
cUAV = Conventional UAV;
IOL = Ideal Operating Line;
ISR = Intelligence Surveillance Reconnaissance;
MAP = Engine Manifold Pressure;

I Introduction

Electric powered Unmanned Aerial Vehicles (UAVs) are not able to achieve their desired range and endurance due to the limited specific energy density of their batteries. Alternatively, the Conventional UAV (cUAV) produce a lot of noise and thermal signatures which make them undesirable especially if the UAV has to patrol at low altitudes and remain undetected by ground patrols.

This work investigates the impact of implementing hybrid propulsion technology to improve on the endurance of a UAV by reducing fuel burn during its mission with implementing a novel control strategy. Various of these control strategies have already been used in the past decades in the automotive industry to reduce the fuel consumption of hybrid vehicles that utilize ICEs and electric motors as a source of propulsion to propel the vehicle (Chan and Chau, 2001; Miller, 2004; Chan *et al.*, 2014; Chan *et al.*, 2002; Ripaccioli *et al.*, 2010; Fengjun *et al.*, 2012; Niels *et al.*, 2003; Cho, 2008; Hu *et al.*, 2004; Donateo *et al.*, 2008; Tran *et al.*, 2021) Some of these techniques includes the usage of a dynamic programming algorithm or model predictive control strategy to minimize the fuel burn emission of Hybrid Electric Vehicles (HEVs) such as gasoline hybrid powertrain vehicles or fuel cell hybrid. Figure 1 shows the various control strategies used in HEVs in the automotive industry.

Each of these controlled methods represents energy management strategies which have been used by previous researchers (Chan *et al.*, 2014; Chan *et al.*, 2002; Ripaccioli *et al.*, 2010; Fengjun *et al.*, 2012; Niels *et al.*, 2003; Hu *et al.*, 2004; Passino *et al.*, 1998) to optimise the fuel consumption of HEVs in the automotive industry. These control strategies are now being used in the aviation industry to reduce the fuel consumption of conventionally powered aircraft and UAVs with an ICE by introducing a more electrified form of propulsion which also have an additional benefit of reducing noise (Dehesa, 2020).

There have been a number of attempts to produce Hybrid-Electric UAVs (Writer, 2020; Ferebee, 2019; Lentsch, 2011; Robertson, 2011; Enviroment, 2012; Hiserote, 2010) RQ-14 Dragon Eye UAV is a small electric reconnaissance UAV used by the U.S. Marine Corps and Helios which is NASA's high-altitude, long endurance UAV powered by solar and fuel cells. The UAV is used for telecommunications and atmospheric monitoring both manufactured by AeroVironment (Writer, 2020). In addition, a hybrid UAV test bed consisting of hydrogen fuel cells and lipo battery was realised by Eskisehir Technical University (Ozbek et al., 2020; Ozbek et al., 2021). Another example is the AAI Aerosonde, which is powered by an Enya R120 engine and is designed to collect weather data such as temperature, pressure and humidity (Writer, 2020). A recent development in electrified powered aircraft is the NASA X-57 Maxwell which makes use of a distributed electric propulsion system consisting of 14 electric motors and propellers to increase the thrust of the aircraft (Ferebee, 2019).

As far as hybrid aircrafts are concerned, the DA-36 E-Star which is the world's first series hybrid-electric aircraft which utilizes a hybrid powertrain in the series configuration has been developed by Siemens and Diamond LTD (Lentsch, 2011). This aircraft was launched for a 1-hour flight at the Paris air show in 2011 and claimed a 25 % reduction in fuel consumption and emission similar to the Eco-Eagle designed by Embry-Riddle Aeronautical University (Robertson, 2011). Another hybrid aircraft in development by Boeing is the SUGAR Freeze that uses liquefied nitrogen fuel cells and electric motor to power an aircraft (Enviroment, 2012). Also, a 13.6 kg UAV with parallel hybrid propulsion has been developed by Air Force Institute of Technology to increase the surveillance time of their current electric powered UAV (Hiserote, 2010).

Some of the advantages of hybridizing (Dehesa, 2020) an aircraft includes:

- Reduction of noise signature through utilizing all-electric propulsion
- Dual capacity providing redundancy in failure in either of the propulsion system
- Reduction in downtime of the aircraft because battery recharging is unnecessary when generator is on board an aircraft

The process of hybridizing an aircraft with electrified forms of propulsion however has a major drawback because of its bulky powertrain due to the increasing weight penalty of the batteries. Therefore, this research explores more sophisticated controlled strategies to hybridize the powertrain of a small UAV.

II Hybrid Powertrain Configuration

A hybrid powertrain is defined here as one that uses energy from two or more power sources to drive the propulsion system where at least one of them delivers electrical energy (Chan and Chau, 2001). This type of configuration is mostly applicable to vehicles. However, with the progress of technology, this concept is now widely used in UAVs to improve their flight time, energy efficiency, and stealth operation for Intelligence Surveillance and Reconnaissance (ISR) missions (Junghsen, 2011). Hybrid-Electric powertrains are broadly classified into 3 categories: Series hybrid, parallel hybrid, and power split (series-parallel) (Jane *et al.*, 2012)

A series hybrid is a type of configuration in which the energy that drives the system comes from the electric motor only. It consists of a fuel tank, an ICE, a generator, a battery, an electric motor, and a drive train which are arranged in series to each other as shown in

Figure 2. The electrical connection shows the flow of electrical energy from the battery to power electronics of the powertrain (i.e electric motor and DC/DC Converter).

Figure 1: HEV powertrain supervisory control strategies reproduced from

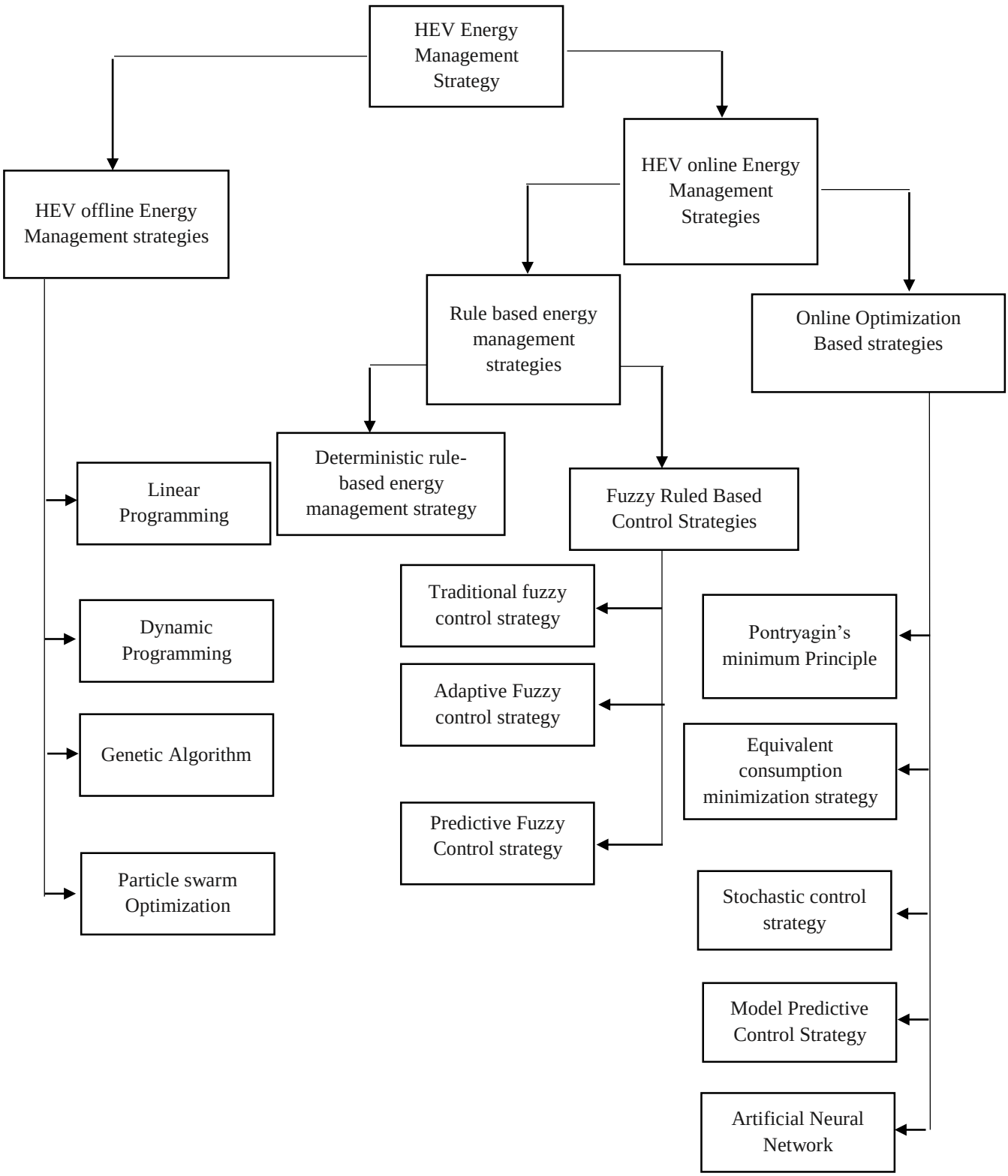

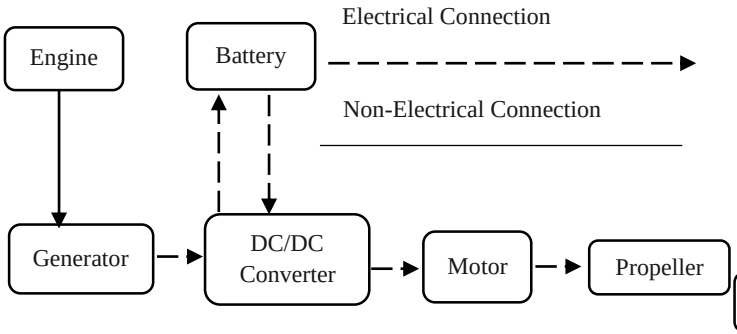

Figure 2: Series hybrid drive train configuration

Meanwhile the non – electrical connection shows the flow of flow of mechanical energy from the engine to generator and transmission. The ICE converts chemical energy from a fuel into mechanical energy which is used to operate the generator. The generator converts mechanical power from the engine into electrical energy which is used to operate the electric motor. The excess energy from the generator is stored in the battery which generally happens when the generator is operating at peak efficiency during periods of low power demand which is then used during periods of high demand (Harmon *et al.*, 2006).The electric motor then converts electrical energy from the generator into a torque that runs the drivetrain. This configuration is, however, not widely used due to the large energy losses associated with numerous power conversions (Harmon, 2005; Ausserer, 2012). Moreover, it requires larger batteries, motors and generators, thus increasing the mass and the volume of the powertrain (Harmon, 2005). This makes the series configuration only suitable for larger vehicles and locomotives (Miller, 2004).

In a parallel configuration shown in Figure 3, both the ICE and electric motor provide power to the drive train. This, therefore, makes the size of its drive train components smaller as compared to the series configuration which makes it useful for most aircraft applications as it imposes less weight penalty.

The series-parallel configuration has characteristics of both a series and parallel configuration which uses a system of planetary gears to transfer power from the ICE and electric motor to the wheels (Figure 4). The main difference between this configuration and other types of configurations is that it uses a set of planetary gears compared to other configurations that are clutch-based. This configuration is, however, not useful for aircraft applications. The disadvantage of using this configuration is the increased mass of the planetary system which makes it heavier than the parallel and series configurations (Jane *et al.*, 2012).

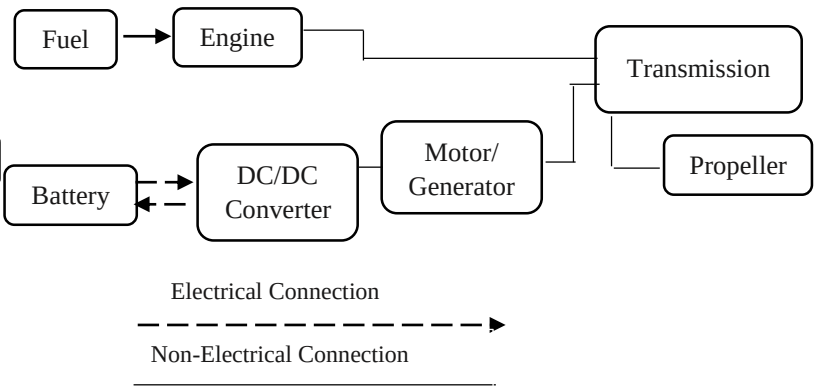

Figure3: Parallel hybrid drive train configuration

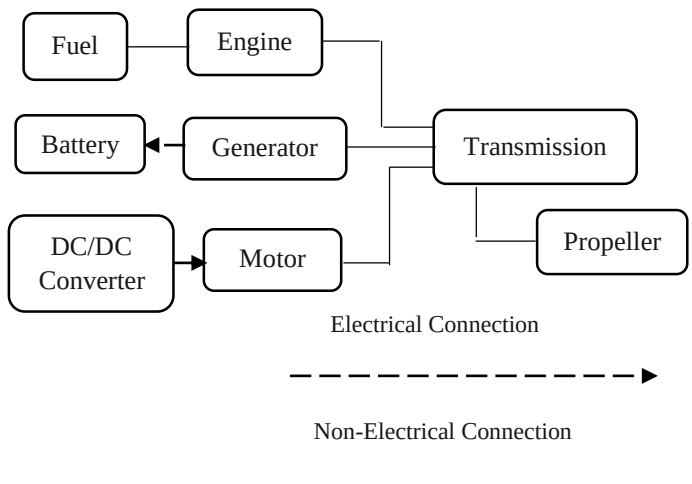

Figure 4: Series - parallel hybrid drive train configuration

III HEPS Modelling

This section describes the modelling of the HEPS as realised in Matlab - Simulink. The modelling of the ICE, Electric Motor, Battery, Propeller and Fuel burn is described. Figure 5 shows a Simulink model representation of the HEPS. The dotted lines represent the input and output variables into and out of each subsystem and are also linked to other subsystems of the HE-UAV while the continuous lines represent variables which link each subsystem of the HEPS.

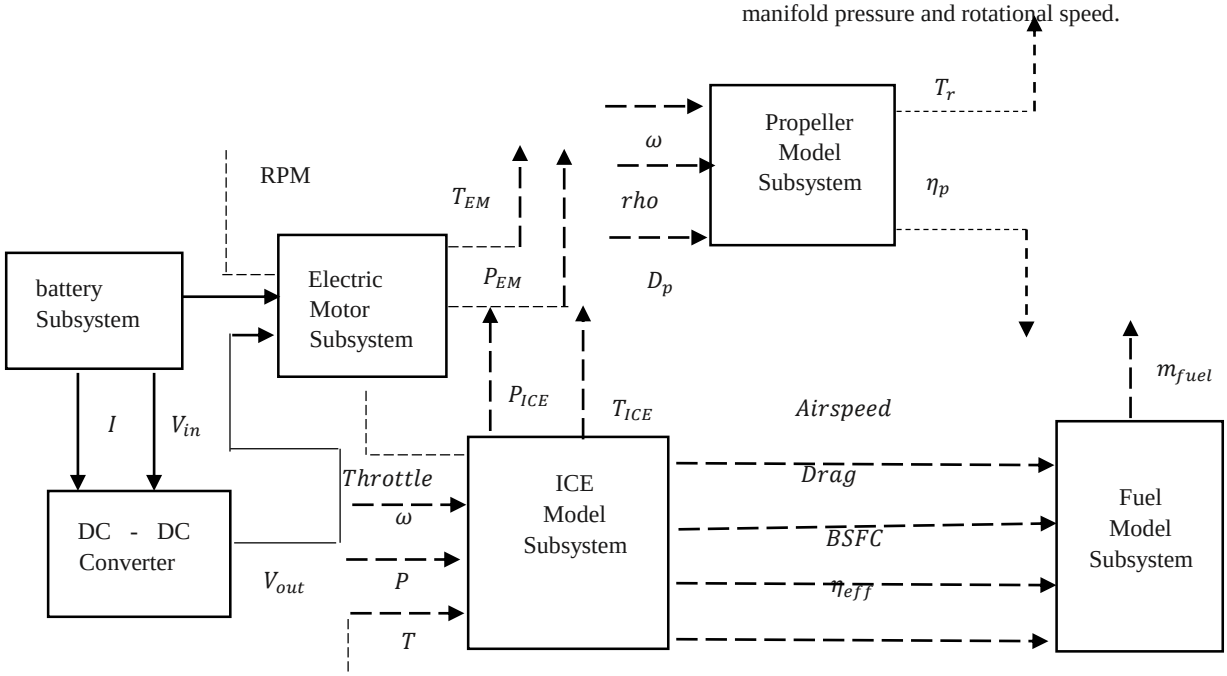

Figure 5: Simulink model of the HEPS

A Battery Model

The battery model was implemented in Matlab - Simulink to model the battery SOC, current and voltage discharge for a given time step. It was done by connecting a Lithium-ion battery cell from the Simulink library developed by MathWorks to a load via a current control source. Lithium-ion battery cell was chosen among the various battery types in Simulink because it has the highest specific energy density. The equations that describe the battery cell dynamics used to create the battery model can be obtained from the math works website (Mathsworks, 2021). The battery model was run for a time step of 3600×6.667 s and was parameterized using a nominal voltage of 24 V and a rated capacity of 14 Ah.

B ICE Model

The ICE was modelled using lookup tables from the Simulink library. It was done using engine data from the Aerosonde UAV obtained from the literature (Gonzalez, 2012). The model determines the engine fuel flow, Brake Specific Fuel Consumption (BSFC), ICE power, ICE torque for a given engine throttle, atmospheric pressure, and engine rotational speed and temperature at a certain reference altitude. The engine manifold pressure (MAP) is determined from the engine throttle (η_{th}) and engine atmospheric pressure (P_{atm}) as:

$$MAP = \eta_{th} * \left(\frac{P_{atm}}{1000} - P_{Min}\right) \qquad (1)$$

The engine conversion block converts the engine speed from Rev/min to rad/s by multiplying the engine rotational speed in rev/min by $\left(\frac{60}{2*Pi}\right)$. The power and fuel flow lookup table determines the ICE power and fuel flow by interpolating a given engine's manifold pressure and rotational speed.

The power and fuel flow data are provided as a function of engine rotational speed and engine manifold pressure, which are used as inputs to create a 2D-lookup table in Simulink to determine the ICE power and fuel flow. The ICE power is multiplied by a correction factor to account for ICE power variation above sea level. The ICE torque is determined by dividing the ICE power with the engine rotational speed. The model is run at various rotational speeds, and the corresponding ICE torque, ICE power and BSFC is recorded from the model by considering various throttle positions of the engine. The data obtained from the model was used to construct the ICE power, torque, brake specific fuel consumption, and engine fuel flow curves in Matlab - Simulink as shown in Figures 6, Figure 7, Figure 8, and Figure 9, respectively.

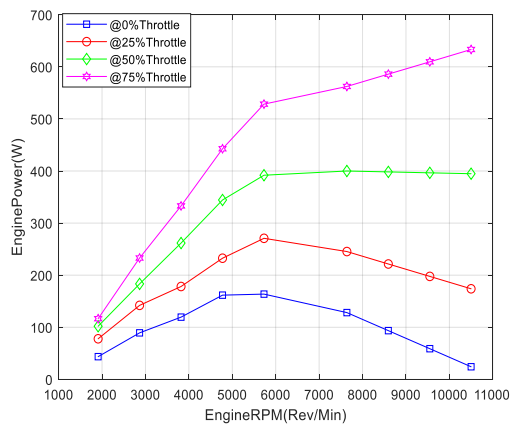

Figure 6: Effect of varying ICE power against engine RPM by considering various throttle positions

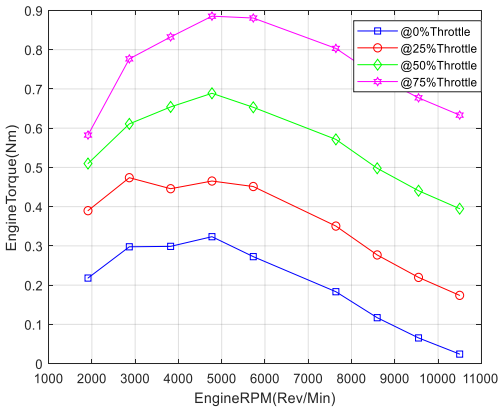

Figure7: Effect of varying ICE torque against engine rotational speed by considering various throttle positions

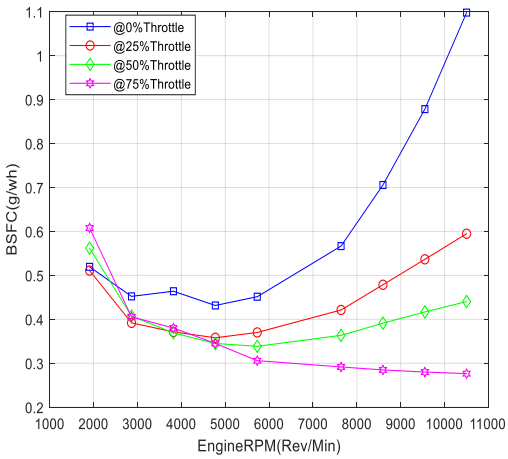

Figure 8: Effect of varying engine BSFC against engine rotational speed by considering various engine throttle positions

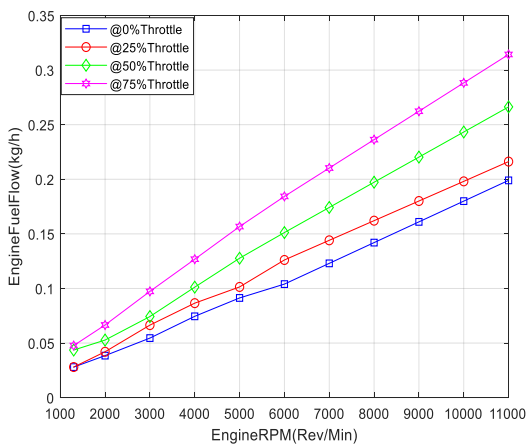

Figure 9: Effect of varying engine fuel flow against engine rotational speed by considering various engine throttle position

The data used in the creation of the ICE Model in Simulink from the Aerosonde UAV is showed in table 1 and 2 respectively.

C Electric Motor Model

The electric motor sub-system was created in Matlab - Simulink using first principles equations which describes the dynamics of a DC motor developed by Drela (Drela, 2007). The DC motor was chosen because of its small size which makes it suitable for HE-UAVs. It models the electric motor power, torque, current, and efficiency for a given motor rotational speed, battery SOC, and voltage. The DC converter is modelled in Matlab - Simulink as an efficiency where it steps down the voltage from the battery subsystem, which is used to drive the electric motor sub-system.
The motor current is determined from the model as:

$$I_m = \frac{\left(U_m - \frac{\Omega}{k_v}\right)}{r_m} \quad (2)$$

Where U_m is the motor terminal voltage, Ω is the motor rotational speed, k_v is the motor speed constant and r_m is the motor internal resistance.

The motor torque is determined from the model as:

$$M_m = \left(\frac{I_m - I_0}{Q_m}\right) \quad (3)$$

Where I_m is the motor current, I_0 is the no load current, Q_m is the motor torque constant.
The motor power is determined by the model by taking the product of motor torque and motor rotational speed as:

$$P_m = M_m \times \Omega \quad (4)$$

Finally, the motor efficiency is determined by the model by taking the ratio of the motor power and electric power into the model as:

$$\eta_m = \frac{P_m}{P_{in}} \quad (5)$$

Where P_{in} is defined as the product of the motor current and terminal voltage from the battery.

$$P_{in} = I_m \times U_m \quad (6)$$

These equations were used to create the electric motor subsystem block model using the Simulink built-in functionalities. The model was parameterized using a nominal voltage of 24 V, a K_v rating of 167 rpm/V, a no-load current of 0.7 A, a torque constant of 0.057 Nm/A and a motor internal resistance of 2.2Ω as obtained from an electric motor datasheet (Motor sheet, 2010).

D Propeller Model

The propeller model sub-system was created in Simulink using APC 6716 propeller performance data from UiUC database (Brandt *et al.*, 2021). It models the propeller thrust, efficiency, and torque for a given propeller diameter, rotational speed, air density, and UAV speed.

The propeller thrust is calculated by the model as:

$$T_r = \rho \times n^2 \times D^4 \times C_T \quad (7)$$

Where: ρ is the air density, n is the rotational speed, D is the propeller diameter and C_T is the propeller thrust coefficient.
The propeller torque is calculated by the model as:

$$T_o = \rho \times n^3 \times D^5 \times C_p \quad (8)$$

Where: C_P is the propeller power coefficient.
Finally, the model calculates the advanced ratio's propeller efficiency by performing a linear interpolation using the Simulink lookup table. The propeller advanced ratio is defined as:

$$J = \frac{V}{nD} \quad (9)$$

Where: V is the air speed of the UAV. Propeller performance data gives propeller thrust coefficient, torque coefficient, and efficiency as a function of advanced ratio, which is implemented using a 1-D lookup table in Simulink. Table 3 shows the parameters used in the creation of the hybrid powertrain in Simulink.

Table 1: Look – Up Table for Engine Fuel Flow from Aerosonde UAV

RPM	MAP								
	60	70	80	90	92	94	96	98	100
1500	31	32	46	53	55	57	65	53	82
2100	40	44	54	69	74	80	92	103	111
2800	50	63	69	92	95	98	126	145	153
3500	66	75	87	110	117	127	150	175	190
4500	83	98	115	143	148	162	191	232	246
5100	93	102	130	159	167	182	208	260	310
5500	100	118	137	169	178	190	232	287	313
6000	104	126	151	184	191	206	253	326	337
7000	123	144	174	210	217	244	321	400	408

Table 2: Look – Up Table for Engine Power from Aerosonde UAV

RPM		MAP							
	60	70	80	90	92	94	96	98	100
1500	18.85	47.12	65.97	67.54	69.12	67.54	67.54	69.12	86.39
2100	59.38	98.96	127.55	149.54	151.74	160.54	178.13	200.12	224.31
2800	93.83	149.54	187.66	237.50	249.23	255.10	307.88	366.52	398.77
3500	109.96	161.27	245.57	307.88	326.20	351.86	421.50	591.14	531.45
4500	164.93	245.05	339.87	438.25	447.68	494.80	565.49	673.87	772.83
5100	181.58	245.67	389.87	496.69	528.73	571.46	662.25	822.47	993.37
5500	184.31	293.74	403.17	535.64	570.20	622.04	748.75	956.09	1059.80
6000	163.36	276.46	420.97	565.49	609.47	691.15	860.80	1131.00	1193.80
7000	124.62	249.23	417.83	586.43	645.07	762.36	996.93	1246.20	1429.40

Table3: Initial parameters of the hybrid powertrain from Simulink

Power Source	**Parameters**	**Values**	**Units**
Battery	Nominal voltage	11.1	V
	Rated capacity	6.3	Ah
	Fully charged voltage	12.9	V
	Cut-off-voltage	8.3	V
	Internal resistance	0.018	Ω
	Capacity at nominal voltage	5.7 [12, 0.31]	A h [V, Ah]
	Exponential zone	100	%
	Initial state of charge		
Electric Motor	Motor idle current	0.7	A
	Rotation speed constant	167	rpm/V
	Motor internal resistance	2.2	Ω
Propeller	Propeller type	APC 6716	m
	Propeller diameter	0.28	
DCDC	Conversion efficiency	0.9	V
	Output voltage	25	
ICE	Sea level temperature	288	K

F Fuel Burn Model

The fuel burn model was created in Matlab - Simulink using equations that govern a reciprocating engine's dynamics from (Anderson, 1999). It models the fuel burn for a given UAV mission for specific fuel consumption, drag, airspeed, and propeller efficiency. The inputs into the model are: the drag force from the UAV model, the airspeed from the mission during simulation, the specific fuel consumption from the ICE model and propeller efficiency from the propeller model. The model's outputs are the fuel burn during simulation and flight time which is read from the simulation clock by the model during the mission. The model calculates the fuel burn rate as:

$$\dot{m_{fuel}} = SFC \times \frac{DV}{\eta_{eff}} \quad (10)$$

The fuel consumption is then calculated at any time step by the model by multiplying the fuel burn rate with simulation time during the mission:

$$m_{fuel} = \dot{m_{fuel}} \times t \quad (11)$$

Where: V is the air speed of the UAV. Propeller performance data gives propeller thrust coefficient, torque coefficient, and efficiency as a function of advanced ratio, which is implemented using a 1-D lookup table in Simulink.

IV 3.3 UAV Model

The UAV model was implemented in Matlab - Simulink using equations for translational flight from Anderson (Anderson, 2012).

$$Tcos\alpha_T - D - Wsin\theta = m\frac{dV}{dt} \quad (12)$$

$$L + Tsin\alpha_T - Wcos\theta = m\frac{V^2}{r_c} \quad (13)$$

where $\frac{dV}{dt}$ and $\frac{V^2}{r_c}$ are the components of the acceleration along the direction of the flight path and normal to the flight path, θ is the angle with respect to the flight path direction (climb angle), α_T is angle with respect to the horizontal (angle of attack). Steady unaccelerated flight was considered i.e $\frac{dV}{dt} = 0$, $\frac{V^2}{r_c} = 0$, level flight was also considered:$\theta = 0$ reducing equation to:

$$Tcos\alpha_T - D = 0 \quad (14)$$
$$L + Tsin\alpha_T - W = 0 \quad (15)$$

With the non-dimensionalised lift and drag coefficient defined as:

$$C_D = \frac{D}{\frac{1}{2}\rho V^2 S_w} \quad (16)$$

$$C_L = \frac{L}{\frac{1}{2}\rho V^2 S_w} \quad (17)$$

The model determines the drag and thrust of the UAV at any given time step during the mission. The inputs to the model are the UAV mass, the air density, the airspeed, the fuel mass, and the altitude. While the outputs of the model are the drag, the thrust, and the angle of climb. The model also has a polar drag curve implemented using polar drag data from the Aerosonde UAV (Dehesa, 2020), which calculates the drag, thrust, and angle of climb at any given time step throughout the mission of the UAV.

V Parallel HE-UAV Controlled Strategy

A rule-based controlled method was used in this research among the various supervisory controlled methods selected from the literature. This was chosen due to its ease of implementation and low computation burden as compared to other supervisory controllers for example, Dynamic Programming. The controller was designed in a Matlab - Simulink environment to switch between the modes of the hybrid powertrain during the mission of the UAV. Figure 10 shows a descriptive flow chart of how the controller operates during the mission of the UAV. The main inputs into the controller are the torque and power coming from both propulsion units of the hybrid powertrain (the ICE and electric motor) and the battery SOC coming from the electric system. An electrification scheme was also introduced to account for the hybridization of the UAV during certain stages of flight of UAV.

Based on the flow chart, the hybrid powertrain has 7 operating modes and at any time during simulation, the supervisory controller has to decide among those modes to determine the output of the hybrid powertrain. i.e the battery SOC during the complete mission of the UAV, it's output torque and power which is summarized in Table 4.

It has as input the total torque and power from the ICE and electric motor model subsystem, the engine fuel flow, engine BSFC, the SOC from the battery model, and electrification parameter. The electrification scheme accounts for the hybridization throughout the mission by calculating the ratio of the electric motor power to the total power from both subsystems. It is defined mathematically as:

$$DOH = \frac{P_{EM}}{P_{ICE}+P_{EM}} \quad (18)$$

Such that during the Conventional Mode:

$$P_{EM} = 0 \text{ and } DOH = 0 \quad (19)$$

During the Electric Mode:

$$P_{ICE} = 0 \text{ and } DOH = 1 \quad (20)$$

During the Hybrid Mode:

$$0 < DOH < 1 \quad (21)$$

Using these inputs, the controller calculates the engine power, engine torque, engine fuel flow, engine BSFC, battery SOC and fuel consumption during the UAV mission.

Table 4: HE-UAV Operating Mode

Operating Mode	Time interval	Phase of the mission	Description of the Mode
Mode 0	750	Take-off + Climb	ICE + electric motor
Mode 1	1250	Cruise	ICE
Mode 2	2000	Endurance	ICE
Mode 3	1000	Cruise	electric motor only
Mode 4	2000	Endurance	ICE
Mode 5	2050	Cruise	electric motor only
Mode 6	750	Descend	ICE

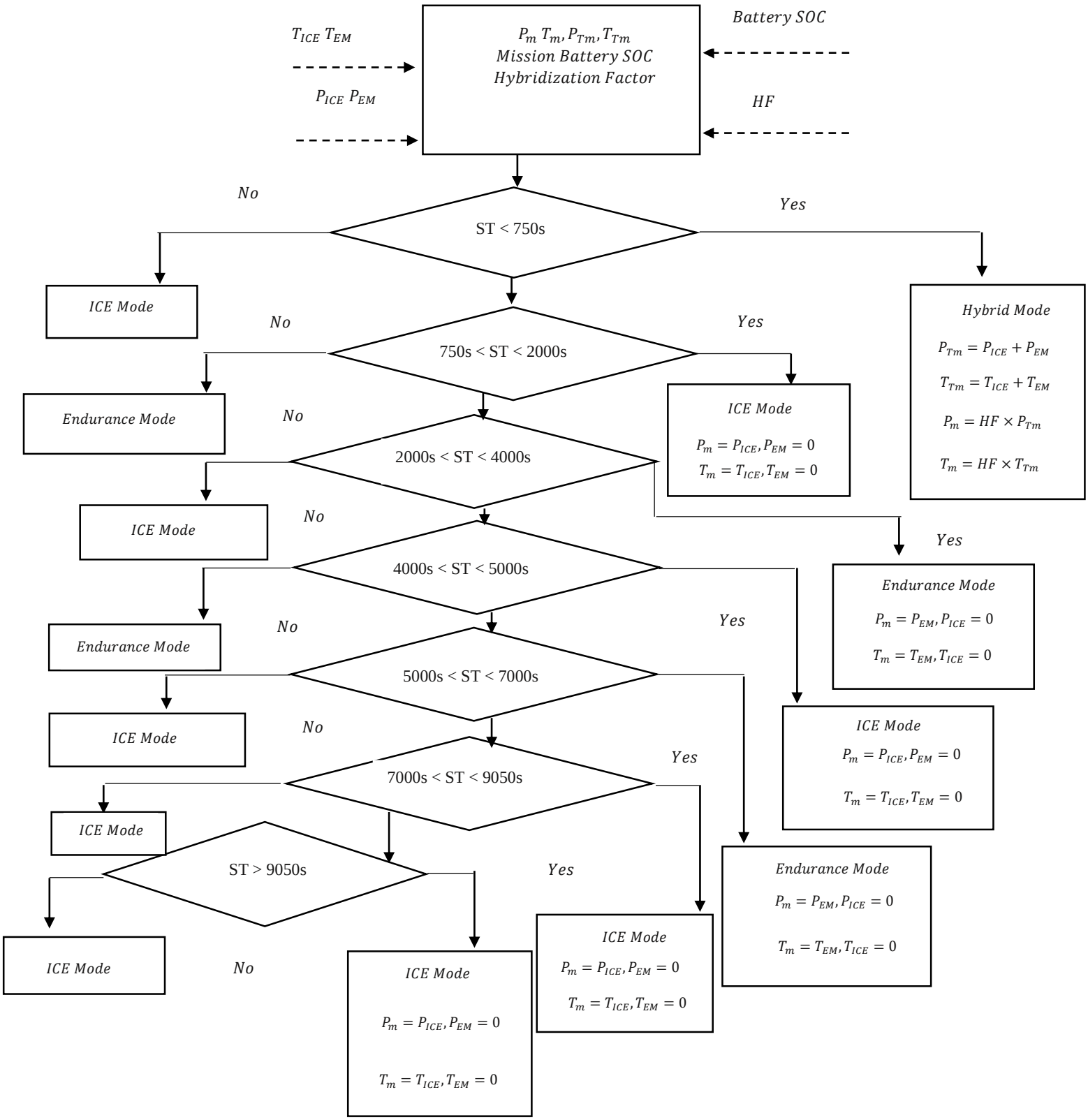

Figure 10: Rule based controlled algorithm flow chart for the split between the ICE and EM

VI Results

An approximately 3h (2.7h) ISR mission used for military application extracted from (Friedrich and Robertson, 2015) was used to simulate the HE-UAV Model developed in Simulink in real time. It consists of seven phases define as:

1. Take-off (750 s)
2. Climb to 1500m (1250 s)
3. Cruise to the location of interest (2000 s)
4. Observe this area at endurance speed (1000 s)
5. Cruise to the location of interest (2000 s)
6. Observe this area at endurance speed (2050 s)
7. Return to the base and land (750 s)

This is represented in Figure 11.

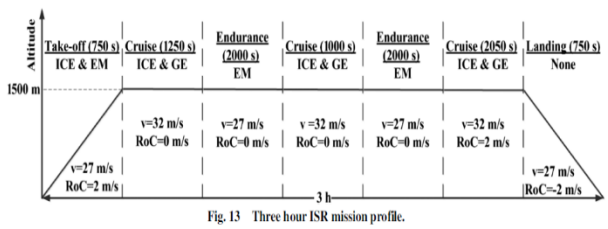

Fig. 13 Three hour ISR mission profile.

Figure 11: Three-hour ISR mission profile

The altitude of the UAV during simulation is 1500 m above sea level, while the cruise and endurance speeds are 32 m/s and 27 m/s respectively as shown in Figure 12 and Figure 13 respectively. Also, during the climb phase the motor rpm reaches a maximum value of 6000 RPM and is kept constant in the successive cruise phases of the mission. Simultaneously in the successive endurance phases when using the electric propulsion system, the rpm drops to 5000RPM as shown in Figure 14. In addition, the rate of climb is kept constant at 10m/s in the climb phase of the mission. Since a steady un accelerated flight was considered, the rate of climb drops to 0m/s in the successive cruise and endurance speed of the mission. In the descend phase of the mission the rate of climb decreases to-10 m/s as shown in Figure 15.

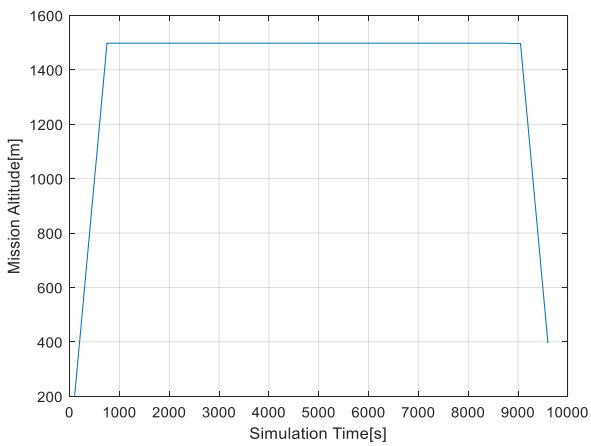

Figure 12: Altitude simulation flight profile

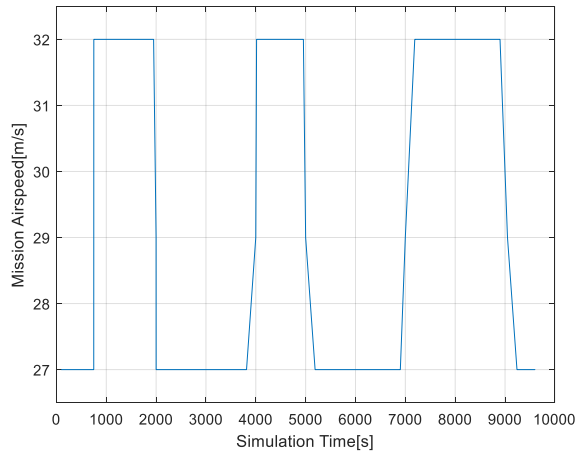

Figure 13: Airspeed simulation flight profile

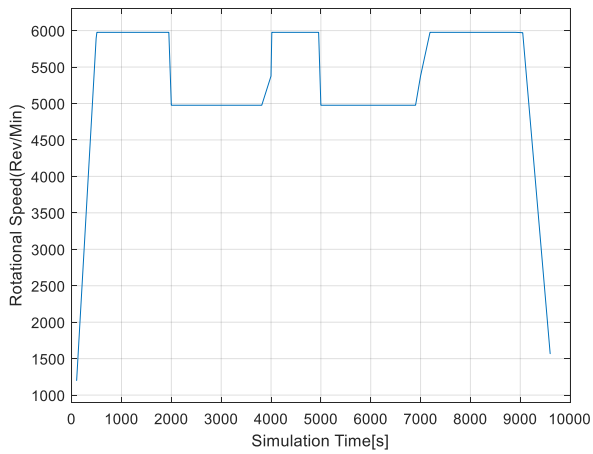

Figure14: Rotational speed simulation flight profile

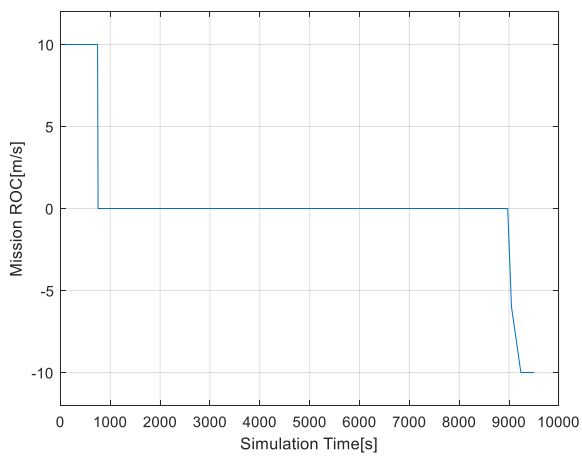

Figure15: Rate of climb simulation flight profile

The effect of implementing the rule based controlled strategy on the hybrid powertrain and conventional model is evaluated. Figure 16 and Figure 17 shows the torque and power output results of the HE-UAV and its comparison to the ICE powered UAV. When the UAV is in hybrid mode, both the hybrid torque and hybrid power increase and reach a maximum value of 0.134 Nm and 409.5 W respectively during the take-off phase (t = 0 s to t = 750 s) of the mission which is due to the increase in RPM from the flight profile curve. During the successive cruise phase of the mission when then the controller switches to ICE mode both the torque and power decreases to 0.047 Nm and 208.1 W respectively and remains constant since the UAV is moving at constant airspeed and RPM from the flight profile curve. In the successive endurance phases of the mission, both torque and power decrease when the controller switches to the electric propulsion system. Finally, in the descend phase of the mission, both the torque and power decreases as the UAV speed and rotational speed decreases from flight profile.

In Figure 18 and 19 the fuel flow and BSFC changes during simulation at various modes are shown respectively. The hybrid mode required less amount of fuel flow than the conventional mode during the climb phase of the mission (0.121 kg/h Vs 0.179 kg/h) as the electrification increases since the UAV uses energy from both the batteries and fuel. Both the fuel flow and BSFC remains constant at 0.125 kg/h and $4.47 \times 10^{-4}\ kg/wh$ respectively during the successive cruise phase of the mission since the UAV moves at constant airspeed and RPM from the flight profile curve. In the endurance phase of the mission when using the electric propulsion system, no fuel is used compared to the approximately 0.14 kg/h and $3.22 \times 10^{-4}\ kg/wh$ during the ICE only configuration.

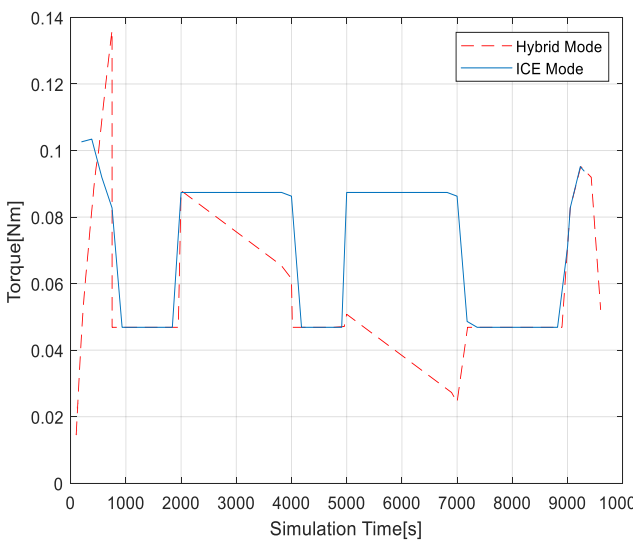

Figure 16: Comparison of Hybrid and ICE torque for a 3h ISR mission profile

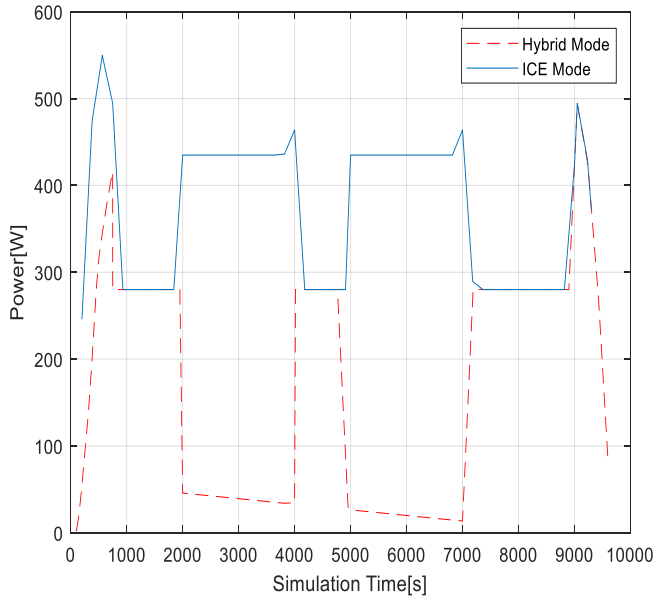

Figure 17: Comparison of Hybrid and ICE power for a 3h ISR mission profile

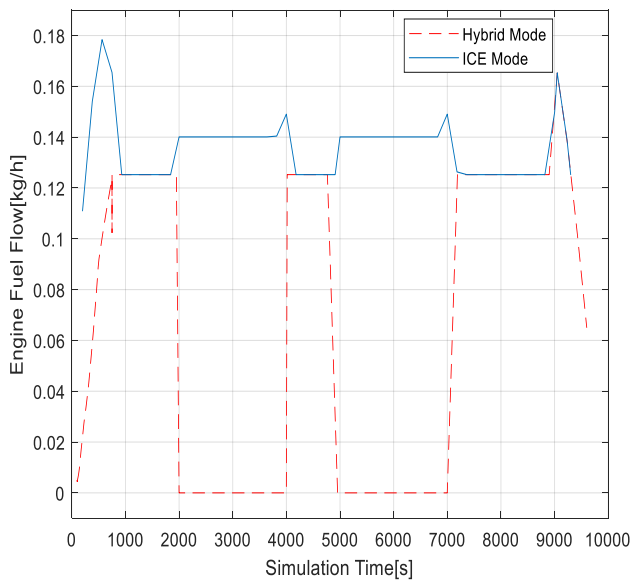

Figure18: Comparison of Hybrid and ICE fuel flow for a 3h ISR mission profile

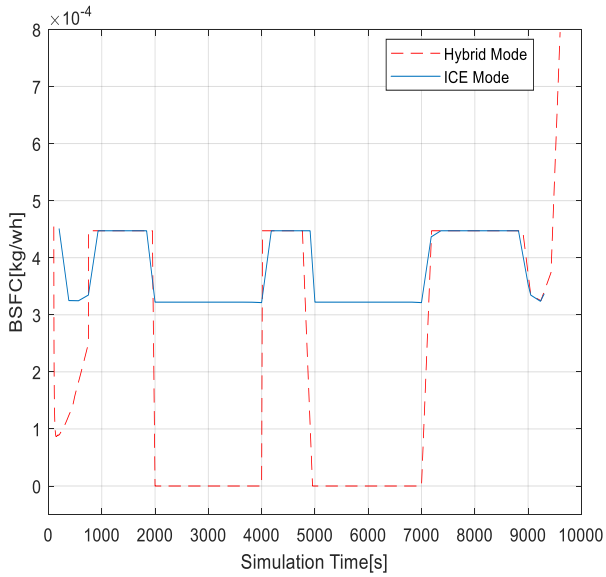

Figure19: Comparison of Hybrid and ICE brake specific fuel consumption for a 3h ISR mission profile

Figure 20 and 21 shows the fuel burn and battery SOC during simulation at various modes respectively. The hybrid mode required a less amount of fuel burn than the conventional mode during the climb phase of the mission. The fuel burn increases during the successive cruise segments of the mission when the ICE is used. While the battery SOC is constant since no power is drawn from the electric propulsion system. In the successive endurance phase of the mission, the fuel burn is constant while the battery SOC decreases

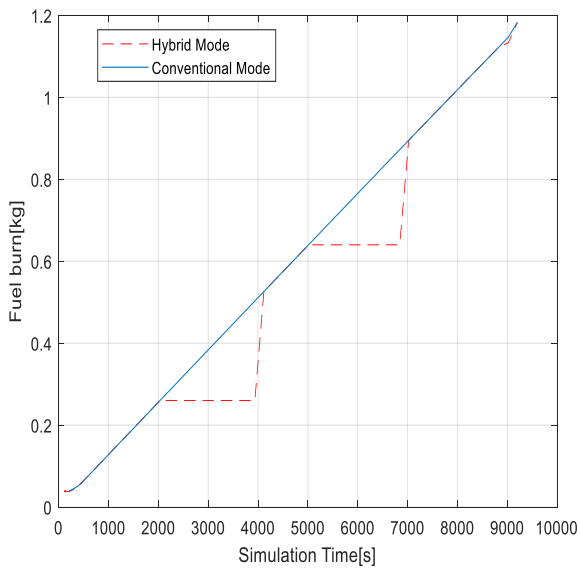

Figure20: Comparison of Hybrid fuel burn with ICE only fuel burn for a 3h ISR mission profile

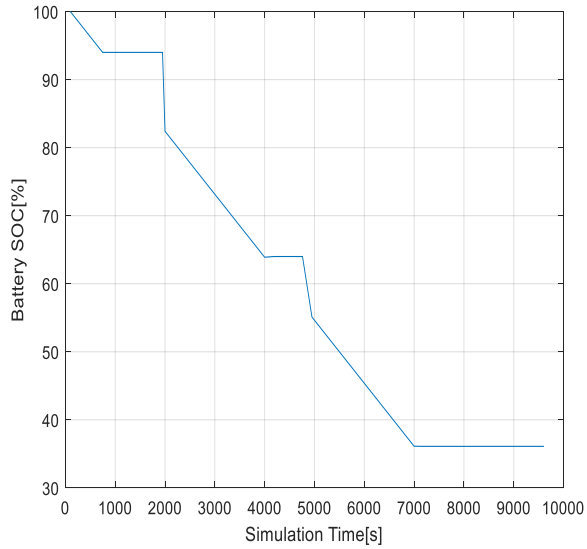

Figure21: Battery SOC for a 3h ISR mission

Figure 22 shows the drag and thrust force results during the flight mission for the HE-UAV and the conventional UAV. During the climb segment, the thrust is slightly higher than the drag at every time step for both modes, with a constant climb angle of 21.7º as shown in Figure 23. For the cruise and endurance phases of the mission both the drag and thrust are the same when the UAV is in steady flight. During the successive cruise and endurance phase the climb angle is zero when the thrust is equal to the drag at every time step during the mission. In the descend phase of the mission, the climb angle is negative when the airspeed of the UAV decreases.

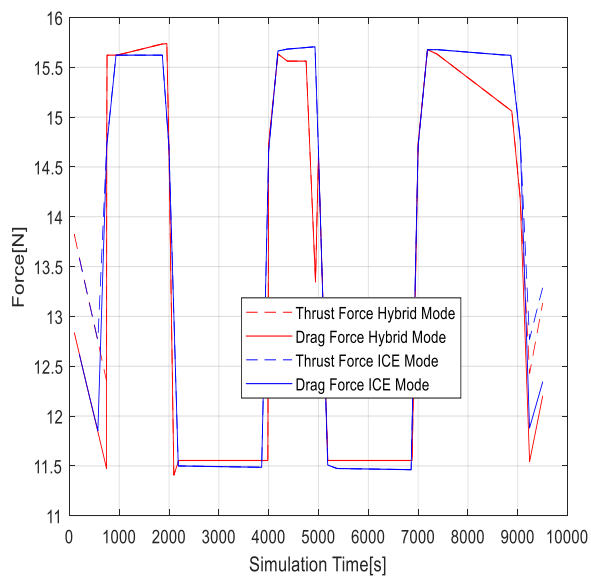

Figure 22: Comparison of Hybrid with ICE only Drag and Thrust Force for a 3h ISR mission profile

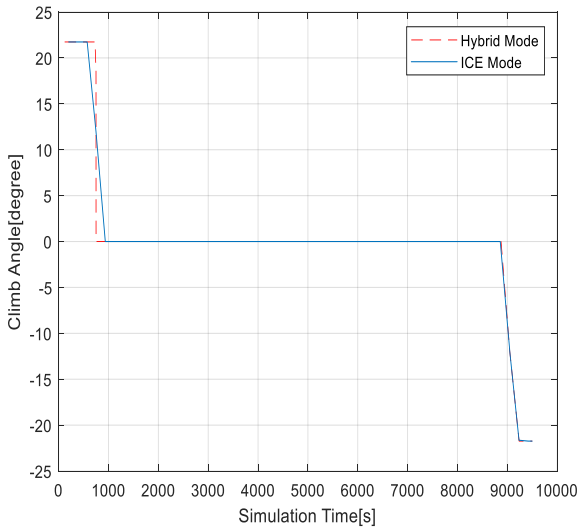

Figure23: Comparison of Hybrid with ICE only climb angle for a 3h ISR mission profile

The effect of electrification on fuel consumption was also analysed during the HE-UAV mission. This was done by varying the time interval during the electric flight of the UAV mission. Table 5 shows the electric mission segments used when defining the mission in Simulink.

Table 5: Mission types with varying degree of electrification

Mission number	Mode	Time Interval
1	2-Electric flight	2000s
	4-Electric flight	2000s
2	2-Electric flight	2500s
	4-Electric flight	3000s
3	2-Electric flight	1500s
	4-Electric flight	1000s
4	Conventional	9500s

Table 6 shows the impact of the varying degrees of electrification on the HE-UAV compared to a UAV with ICE only. The HE-UAV consumes less fuel when the electrification is increased with the least fuel consumption of 0.64kg when the electrification was 56.1 %. Also, the UAV consumes more fuel when the electrification is decreased with the highest fuel consumption of 0.95 kg when the electrification is 25.51 %. The HE-UAV shows a potential fuel saving of 33 % compared to the conventional mode when mission 1 is used followed by 56.1 % and 19.5 % for mission 2 and mission 3 respectively.

Table 6: Sizing of a 3 h ISR for a HE-UAV with vary degree of electrification

Electrification %	**40.8 (Mission1)**	**56.1 (Mission 2)**	**25.5 (Mission 3)**	**0 (Mission 4)**
Empty weight, kg	4.9	4.9	4.9	4.9
Engine weight, kg	4.1	4.1	4.1	4.1
Motor Weight, kg	2.3	2.3	2.3	2.3
Fuel Weight (HE-UAV), kg	0.79	0.64	0.95	-
Fuel Weight, kg (Conventional Mode)	1.18	1.18	1.18	1.18
Battery weight, kg	1.6	1.6	1.6	1.6
Payload weight, kg	0.6	0.66	0.66	0.66
Total Weight, kg	13.6	13.6	13.6	13.6
Fuel Saving with reference to the conventional mode	33.0%	45.8 %	19.5%	-

A simple sizing function was also implemented to determine the weight of the various powertrain components for the given mission after evaluating the fuel consumption of each mission as shown in Table 6.

Validation of the model was done using the same inputs of the model with that of the Aerosonde UAV (Aerosonde datasheet, 2021). Table 7 shows the inputs used on the HE-UAV Simulink model and that of the Aerosonde UAV. Figure 24 shows the fuel burn results for the conventional mode for user specified inputs to the model. Based on the given inputs, the results of the simulation show that the conventional UAV consumed about 1.01 kg of fuel for a 2.5 hr ISR mission. According to (Aerosonde datasheet, 2021). An Aerosonde UAV consumes about 1.5 U. S gallons the equivalence of 5.7 kg of fuel for a 15 h and 45 minutes mission'. By proportion, it means that the actual UAV will consume about 0.922 kg of fuel for a 2.5 hr mission. This gives a percentage increase of 9.5 % compared to the real UAV mission.

Table 7: Inputs to Simulink model from Aerosonde UAV

Parameters	Aerosonde UAV	Simulink Model	
Wing Span(m)	2.9	2.9	
Weight(kg)	13.1	13.1	
Endurance(hr)	14+	14+	
Airspeed (m/s)	20	20	
Wing loading(kg/m^2)	23	23	
Wing Area(m^2)	0.57	0.57	

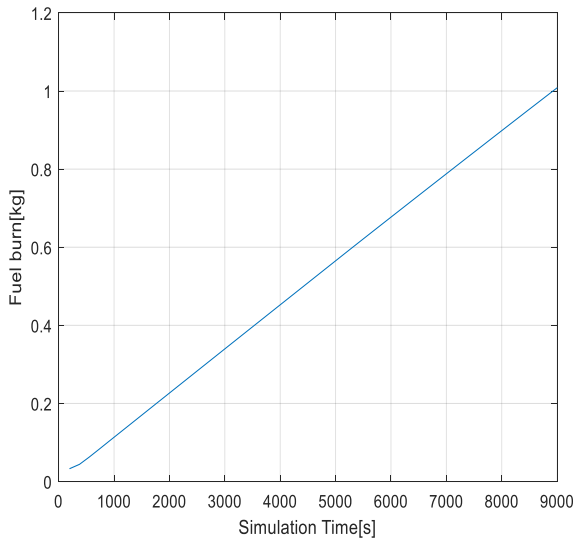

Figure 24: Fuel consumption results for the conventional UAV using the Aerosonde UAV inputs data

VII Conclusion

Generally, in the aviation industry, the goal is to design high performance aircrafts which are efficient in fuel saving cost. In this thesis, the impact of implementing hybrid propulsion technology to improve on the endurance of a UAV by reducing fuel burn during its mission was investigated through the implementing a novel control strategy. This was achieved by creating a HE-UAV model to analyse the fuel saving cost of a 13.6 kg UAV for a given mission profile (3 h ISR) which was then compared to a conventional UAV. The model can also be used to analysed the fuel saving cost of any UAV configuration of similar take-off weight for any given mission profiles. A supervisory controller is implemented to characterise the split between the ICE and electric motor during the UAV mission which using a rule based controlled strategy. The controller allows the UAV to use ICE power or electric only power or a combination of the two during the UAV mission.

An electrification scheme is implemented to account for the hybridization of the UAV during certain stages of flight. The electrification scheme is then varied by changing the time duration of the UAV during certain stages of flight meaning, when the UAV is in electric mode and the fuel consumption during each mission is determined and compared to the conventional mode.

Based on simulation, itis observed a HE-UAV could achieve a fuel saving of 33 % compared to the conventional mode. In order to account for the relative weight of the components during a given UAV mission, a simple sizing code was developed to determine the size of the various powertrain components after analysing the fuel consumption of the UAV for given mission profiles.

A validation of the model using manufacturer data and information on the flying mission of the Aerosonde UAV was done to make some deductions from this model. The simulated results estimated an approximated fuel saving of 9.5 %.

Some suggestions to improve on the existing work might be to:

- Investigate on the effects of wind and weather conditions on the performance of the HE-UAV model.
- Exploring more advanced controllers and performing various optimization techniques on certain mission segments to minimize on the fuel consumption of the UAV in order to improve on its fuel economy.
- An experimental work could be done by constructing a small prototype of a HE-UAV using commercial off the shelf products to test the developed algorithm in real time.

References

Anderson, J.D. (1999), Aircraft Performance and Design, McGraw-Hill, Boston, MA.

Anderson, J.D. (2012), Introduction to Flight, McGraw-Hill, Boston, MA.

Ausserer, A. (2012), "Integration, Testing, and Validation of a Small Hybrid-Electric Remotely-Piloted Aircraft", *Master's Thesis*, Air Force Institute of Technology.

Bertsekas, D. P. (1995), Dynamic Programming and Optimal Control, Belmont, MA Athena Scientific.

Bagassi, S., Bertini, G., Francia, D. and Persiani, F. (2012), "Design Analysis For Hybrid Propulsion", *28th International Congress of the Aeronautical Sciences*.

Brandt, J.B., Deters, R.W., Ananda, G.K., Dantsker, O.D. and Selig, M.S. (2021), " UIUC Propeller Database", Vols 1-3, University of Illinois at Urbana-Champaign.

Chen, D. (2016), "Implementation of Dynamic Programming and Its Application to an HEV", *Energies*, Vol. 8 No. 4, pp. 3225-3244

Chan, L., Peng, H., Grizzle, W., Jason, L., Busdiecker, M. and Worth, F. (2014), "Control System Development for an Advanced-Technology Medium-Duty Hybrid Electric Truck", *SAE transactions*, pp.105-113.

Chan, C.C. and Chau, K.T. (2001), "Modern Electric Vehicle Technology", Oxford University Press, Oxford, England, U.K.

Chan, L., Filipi, Z., Wang, Y. and. Louca, L. (2002), "Integrated, Feed-Forward Hybrid Electric Vehicle Simulation in SIMULINK and Its Use for Power Management Studies", *SAE Technical Paper*.

Cho, B. (2008), "Control of a Hybrid Electric Vehicle with Predictive Journey Estimation", Ph.D. Thesis, Cranfield University, Cranfield, UK.

Danielle, M., Alexander, R. and Wang, J. (2018), "A Simple Method for Energy Optimization to Enhance Durability of Hybrid UAV Power Systems", In *North American Power Symposium* (NAPS), pp. 1-6.

Dehesa, D.A. (2020), "Study of Control Schemes for Series Hybrid – Electric Powertrain For Unmanned Aerial Systems" *Master's Thesis Lousiana State University, Lu*.

Donateo, T., Serrao, L., Rizzoni, G. (2008), "A Two-Step Optimisation Method for the Preliminary Design of a Hybrid Electric Vehicle", *International Journal of Electric and Hybrid Vehicles*, Vol. 1, No 2, pp. 142-165.

Drela, M. (2007), "First-Order DC Electric Motor Model", Technical Report, Aero and Astro, MIT.

Drela, M. (2007), "Second-Order DC Electric Motor Model", Technical Report, Aero and Astro, MIT.

Drela, M. (2005), "DC Motor/Propeller Matching", Lab 5 Lecture notes.

Electric Motor Performance Datasheet HT-POG36-1211522.

Passino, K.M., Yurkovich, S. (1998), Fuzzy Control, Addison-Wesley.

Enviroment, I. (2012), SUGAR Volt: Boeing's Hybrid Electric Aircraft, Viewed 5 may 2021, < https://www.boeing.com/features/2012/05/sugar-volt-boeing-hybrid-electric-aircraft-05-2-12.page >

Eleftherios, A., Tsili, M., and Spathopoulos,V. (2014), "Energy Efficiency Optimization in UAVs: A Review", *In Materials Science Forum* , Vol. 792, pp. 281-286.

Fengjun, Y., Wang, J. and Kaisheng, H. (2012), "Hybrid Electric Vehicle Model Predicitive Control Torque-Split Strategy Incorporating Engine Transient Characteristics", IEEE transactions on vehicular technology, Vol 61, No 6, pp.2458-2467.

Ferebee, M. (2019), X-57 Maxwell, Viewed 3 March 2020, < https://sacd.larc.nasa.gov/x57maxwell/ >

Friedrich, C. and Robertson, P.A. (2015), " Hybrid-Electric Propulsion for Aircraft",Vol 52, No 1.

Harmon, F. (2005), "Neural Network Control of a Parallel Hybrid- Electric Propulsion System for a Small Unmanned Aerial Vehicle", *PhD Thesis*. University of California Davis, California.

Gonzalez, Y. (2012), "Design, Simulation and Analysis of a Parallel Hybrid Electric Propulsion System for Unmanned Aerial Vehicles", Proceedings of the 28th Congress of the International Council of the Aeronautical Science - ICAS, Vol 51 pp. 1-7.

Harmon, F. A., Frank, A.A. and Chattot, J. (2006), "Conceptual Design and Simulation of a Small Hybrid-Electric Unmanned Aerial Vehicle", *Journal of Aircraft*, Vol 43, No 5, pp.1490-1498.

Harmats, M. and Weihs, D. (1999), "Hybrid-Propulsion High Altitude Long-Endurance Remotely Piloted Vehicle", *Journal of Aircraft*, Vol 36, No 2, pp. 321 – 331.

Hu, X., Wang, Z., Liao, L. (2004), "Multi-Objective Optimization of HEV Fuel Economy and Emissions using Evolutionary Computation.", SAE Technical Paper, pp. 117-128.

Jane, Y., Felipe, L., Chun, J. and Gonzalez, L. (2012), "On Parallel Hybrid-Electric Propulsion System for Unmanned Aerial Vehicles", Progress in Aerospace Sciences, Vol 51, pp.1-17.

Jeremy, T. and Kraig, R. (2011), "Conceptual Design of Low - Signature High - Endurance Hybrid-Electric UAV", Institute For Defense Analyses.

Junghsen, L. (2011), "Design of Hybrid Propulsion Systems for Unmanned Aerial Vehicles", *47th AIAA/ASME/SAE/ASEE Joint Propulsion Conference & Exhibit p. 6146*.

Keidel, B. (2000), "Design and Simulation of High-Flying, Permanently Deployable Solar Drones", *Ph. D. Thesis*, Technische Universität München.

Lentsch, A. (2011), "Diamond Aircraft Proudly Presents the World's First Serial Hybrid Electric Aircraft "DA36 E-Star" Viewed 3 March 2020, < https://www.diamondaircraft.com/en/about-diamond/newsroom/news/article/diamond-aircraft-proudly-presents-the-worlds-first-serial-hybrid-electric-aircraft-da36-e-star/ >.

Luigi, S. and Placentino, D. (2017), "Design and Performance Evaluation of a Hybrid Electric Power System for Multicopters", *Energy Procedia*, Vol. 126, pp. 1035–42.

Lithium-Ion Battery datasheet 15-24-1000.

Rippel, M. (2011), "Sizing Analysis For Aircraft Utilizing Hybrid-Electric Propulsion Systems", *Master's Thesis*, Air Force Institute of Technology, OH.

Martin, J. and Adair, D. (2017), "Conceptual Design of a High-Endurance Hybrid Electric Unmanned Aerial Vehicle", *Materials Today*: Proceedings , Vol 4, No 3, pp 4458–68.

Miller, J. (2004), "Propulsion Systems for Hybrid Vehicles", *IEE Power & Energy Series*, IEE, London, UK.

Murat, B., Moschetta, J. G., Hattenberger, Bronz, M., Moschetta, J. and Hattenberger, G. (2014), "Multi-Point Optimisation of a Propulsion Set as Applied to a Multi-Tasking MAV", International Micro Aerial Vehicle Conference and Competition.

Nam, T., Soban, D.S. and Mavris, D.N. (2005), "A Generalized Aircraft Sizing Method Application to Electric Aircraft", *3rd International Energy Conversion Engineering Conference*, Georgia Institute of Technology, Atlanta.

Niels, S., Mutasim, J., Salman, A and Kheir, N. (2003), " Emissions and Fuel Economy Trade-Off for Hybrid Vehicles Using Fuzzy Logic", Mathematics and Computers in Simulation Journal, Vol 66, No. 2-3, pp.155-172.

Ozbek, M., Yalin, G., Ekici, S., Karakoc, T.H.(2020),"Evaluation of design methodology, limitations and iterations of a hydrogen fuelled hybrid fuel cell mini UAV", Energy , 213, p.118757.

Ozbek, M., Yalin, G., Ekici, S., Karakoc, T.H.(2021), " Architecture Design and Performance Analysis of a Hybrid Hydrogen Fuel Cell System For Unmanned Aerial Vehicle", International Journal of Hydrogen Energy, Vol 46, No 30, pp. 16453 - 16464.

Pornet, C., Gologan, C., Vratny, P.C., Seitz, A., Schmitz, O., Isikveren, A.T. and Hornung, M. (2015), "Methodology for Sizing and Performance Assessment of Hybrid Energy Aircraft", Journal of Aircraft, Vol 52, No 1.

Riboldi, C.E.D. (2018), "An Optimal Approach to the Preliminary Design of Small Hybrid-Electric Aircraft", Aerospace Science and Technology, Vol 81, pp. 14–31.

Riboldi, C.E.D., Gualdoni, F. and Trainelli, L. (2018), "Preliminary Sizing of a Light Pure-Electric and Aircraft Preliminary Weight Sizing and Hybrid-Electric", *Transportation Research Procedia*, Vol 29, pp376–89.

Richard, R., Jane, Y., Luis, F., Glassock, R., Hung, J., Gonzalez, F. and Walker, A. (2009), " Multimodal Hybrid Powerplant for Unmanned Aerial Systems (UAS) Robotics", In *Proceedings of the Twenty-Fourth Bristol International Unmanned Air Vehicle Systems Conference*, pp. 1-13.

Ripaccioli, G., Bernardini, D., Cairano, D., Bemporad, A. and Kolmanovsk, I. (2010), "A Stochastic Model Predictive Control Approach for Series Hybrid Electric Vehicle Power Management " , *In Proceedings of the 2010 American Control Conference*, pp. 5844-5849.

Robertson, D. (2011), Embry-Riddle 95th Anniversary Edition Alumni Directory, Viewed 3 March 2020, <https://alumni.erau.edu/s/867/bp20/interior.aspx?sid=867&gid=1&calcid=4036&calpgid=61&pgi]d=252&ecid=2426&crid=0 >

Hiserote, R. (2010), " Analysis of Hybrid-Electric Propulsion System Design For Small Unmanned Aircraft Systems", *Master's Thesis.* Air Force Institute of Technology, OH.

Salento, S. (2018), "A Method to Analyze and Optimize Hybrid Electric Architectures Applied to Unmanned Aerial Vehicles", Aircraft Engineering and Aerospace Technology. J. Aerosp. , Vol 10, No. 1, pp.12-20.

https://www.mathworks.com/help/physmod/sps/powersys/ref/battery.html.

Savvaris, A., Laycock, J. and Farmer, A. (2018), "Modelling and Control of a Hybrid Electric Propulsion System for Unmanned Aerial Vehicles", IEEE Aerospace Conference, pp. 1-13.

Schneider, K.K., Sausen , P.S. and Sausen, A. (2011), "Comparative Analysis of Battery Life in Mobile Devices Using Analytical Models", *TEMA-Tend. Applicable Mat. Computer*, Vol 12, No. 1, pp. 43-54.

Schömann, J. (2014), "Hybrid Electric Propulsion Systems for Small Unmanned Aircraft", *Master Thesis*, Technische Universität München.

Schoemann, J. and Hornung, M. (2012), "Modelling of Hybrid-Electric Propulsion Systems for Small Unmanned Aerial Vehicles", *12th AIAA Aviation Technology, Integration and Operations and 14th AIAA/ISSMO Multidisciplinary Analysis and Optimization Conference, p. 5610.*

Schoemann, J. and Hornung, M. (2013), "Design of Hybrid-Electric Propulsion Systems for Small Unmanned Aerial Vehicles", *5th European Conference for Aeronautics and S"pace Sciences*, Munich, Germany.

Schalkwyk, J. v. (2018), "Redesign and Optimization of the MWEWE UAV for Improving in Aircraft Endurance", BEng Honours Report, University of Pretoria, Pretoria, South Africa.

Sliwinski, J., Alessandro, G., Matthew, M., and R. Sabatini. (2017), "Hybrid-Electric Propulsion Integration in Unmanned Aircraft Hybrid-Electric Propulsion Integration in Unmanned Aircraft", *Energy*, Vol 140, No. 2, pp. 1407-1416.

Taewoo, N., Soban, S. and Mavris, N. (2005), "Power Based Sizing Method For Aircraft Consuming Unconventional Energy", *43rd AIAA Aerospace Sciences Meeting and Exhibit, p. 818*.

Donateo, T. and Ficarella, A. (2017), "Designing a Hybrid Electric Powertrain for a Unmanned Aircraft with a Commercial Optimization Software", SAE International Journal of Aerospace, Vol 10, No 1, pp.1-11.

Donateo, T. and Spedicato, L. (2017), "Fuel Economy of Hybrid Electric Flight", *Applied Energy*, Vol 206, pp723-738.

Rotramel, T. (2011), "Optimization of Hybrid-Electric Propulsion System for Small Remotely-Piloted Aircraft", *Master's Thesis.* Air Force Institute of Technology, OH.

Tomaselli, M., Monopoli, G. and Cupertino, F. (2017), "Hybrid Aeronautical Propulsion Control and Energy Management", *IFAC-PapersOnLine, Vol 50, No. 2 pp.169-174.*

Tran, M., Akinsanya, M., Panchal, S., Fraser, R. (2021), "Design of a Hybrid Electric Vehicle Powertrain for Performance Optimization Considering Various Powertrain Components and Configurations", Vehicles, Vol 3, pp 20–32.

https://en.wikipedia.org/w/index.php?title=AAI_Aerosonde&oldid=1026399344.

Wall, T. (2017), "Model Predictive Power Management of a Hybrid Electric Propulsion System for Aircraft", Master's Thesis, Western Michigan University.

Voskuijl, M. (2018), " Analysis and Design of Hybrid Electric Regional Turboprop Aircraft", *CEAS Aeronautical Journal*, Vol 9 No 1, pp 15–25.

Wikipedia Contributors August 13 2021, Simulink, In Wikipedia, The Free Encyclopedia. Retrieved 12:54, https://en.wikipedia.org/w/index.php?title=Simulink&oldid=1038594091.

Zang, X., Liu, L. and Dai, Y. (2018), "Fuzzy State Machine Energy Management Strategy for Hybrid Electric UAVs with PV / Fuel Cell / Battery Power System", *International Journal of Aerospace Engineering*.

Xie, Y., Savvaris, A. and Tsourdos, A. (2019), "Fuzzy Logic Based Equivalent Consumption Optimization of a Hybrid Electric Propulsion System for Unmanned Aerial Vehicles", *Aerospace Science and Technology*, Vol 85, pp.13-23.

.